A Comparison of GADRAS-Simulated and Measured Gamma-ray Spectra

Ron Jeffcoat, Saleem Salaymeh, Aaron Clare
Savannah River National Laboratory

ABSTRACT

Gamma-ray radiation detection systems are continuously being developed and improved for detecting the presence of radioactive material and for identifying isotopes present. Gamma-ray spectra, from many different isotopes and in different types and thicknesses of attenuation material and matrixes, are needed to evaluate the performance of these devices. Recently, a test and evaluation exercise was performed by the Savannah River National Laboratory that required a large number of gamma-ray spectra. Simulated spectra were used for a major portion of the testing in order to provide a pool of data large enough for the results to be statistically significant. The test data set was comprised of two types of data, measured and simulated. The measured data were acquired with a hand-held Radioisotope Identification Device (RIID) and simulated spectra were created using Gamma Detector Response and Analysis Software (GADRAS, Mitchell and Mattingly, Sandia National Laboratory). GADRAS uses a one-dimensional discrete ordinate calculation to simulate gamma-ray spectra. The measured and simulated spectra have been analyzed and compared. This paper will discuss the results of the comparison and offer explanations for spectral differences.

INTODUCTION

GADRAS[1] (GAmma Detector Response and Analysis Software) is a powerful gamma-ray spectral analysis software toolset developed at Sandia National Laboratories (SNL). GADRAS performs a full-spectrum analysis, not just a full-energy peak analysis**.** It can be used in analyzing gamma-ray spectra from sodium iodide and high purity germanium (HPGe) detector instruments. GADRAS is widely used across the DOE complex to analyze unknown gamma-ray spectra acquired from a variety of handheld, portable and larger fixed systems such as portal monitors. There are many analysis tools available for modeling source to detector configurations such as the GGH (generalized geometry holdup) model, MCNP, Isotopic, ISOCS, Gammavision and others[2]. GADRAS has been proven to be a state-of-the-art, user-friendly, yet powerful analysis and modeling tool for gamma-ray spectrocopists. It is easy to use and analyses can be set up and performed rapidly.

GADRAS was very useful in a project funded by the Nonproliferation Detection program of NA-22[3]. The primary goal of the project was to bring successful technology from other areas of signal processing expertise into the field of radioisotope identification using gamma-ray spectroscopy. These new algorithms[4,5] addressed the problem of detection and classification techniques to provide high confidence gamma spectrum analysis, especially for shielded and masked SNM/RDD (Special Nuclear Material/Radiological Dispersal Devices) materials.

This project required experimentally acquiring gamma-ray spectra with actual sources and simulating gamma-ray spectra using the GADRAS inject data function. These spectra were created under well-controlled, documented conditions such as radionuclide activity, source-to-detector distance, background radioactivity levels and various types and thicknesses of attenuating materials. During early phases of the project, spectra were acquired for long counting times as the data were used for energy calibration, detector characterization and algorithm development. Gamma-ray spectra used for the Test and Evaluation[6] were acquired for 60 seconds live time and under challenging conditions to emulate realistic field data. Some of the measured gamma spectra were treated as unknown sources and were analyzed with GADRAS to provide validation and confirmation that this software toolset can be used to accurately determine source strength and isotope identification. A detailed explanation of the methodology used in supplying gamma-ray spectra for the project are discussed in this paper, including data acquisition, GADRAS modeling and simulations and GADRAS analysis results.

METHODOLOGY

Detector characterization

In order to ensure the instrument was optimized and to create high quality gamma-ray spectra, both measured and simulated, it was necessary to characterize the instrument by generating a good detector response function. This is necessary for accurately analyzing data and comparing results. The instrument used in this study was a low resolution NaI detector (Identifinder NGH). Gamma-ray spectra were acquired in well-controlled geometries using well-characterized sources that emit gamma rays with energies between 60 and 3000 keV. The six isotopes designated with an asterisk in Table 1 were measured at a distance of 50 centimeters, giving a broad energy range for the detector characterization. Acquisition times ranged from 900 to 57,600 seconds so that at least 10,000 counts were observed in each gamma-ray photopeak of interest. Table 1 also shows source identification numbers and source activities for all sources used in this study.

Table 1: Sources Used for Measurements

Source #	Isotope	Source I.D.	Activity (uCi)	Live Time (Det.Char.)
1	Co-60	1235-28-1	7.1	
2 *	Co-60	1235-28-2	6.9	1800
3 *	Co-57	1235-27-1	3.7	1800
4	Co-57	1235-27-2	3.9	
5 *	Ba-133	1235-29-1	32.4	900
6 *	Cs-137	1235-30-1	46.2	900
7	Cs-137	1235-30-2	46.5	
8 *	Am-241	1233-52-1	50.2	900
9	Am-241	1209-61-1	47.2	
10 *	Th-228	720-16-2	0.27	57600
11	Eu-152	720-15-3	6.7	
12	Bi-207	720-16-1	7.8	
13	Mn-54	na	0.086	
14	Na-22	ns	0.209	
15	Ra-226	1233-52-2	10.7	
* sources used for detector charaterization				

Experimental Data

The measured gamma-ray spectra used for this study were acquired with a low resolution NaI detector for various live times that range from one minute to many hours. The instrument was an Identifinder NGH detector that was located 1 meter up from the floor. To minimize scatter from surrounding objects, the aluminum frame measurement apparatus, shown in Figures 1 and 2, was located in the center of a room at least four feet from a wall or other large structures. A plexiglas shelf can be seen at one end of the frame, and at the horizontal center of the frame is a platform for the detector and a removable, vertical Plexiglas positioning plate. This configuration was maintained throughout this measurement campaign to strive for consistency of detector response and minimal backscattering.

Figure 1: Measurement Apparatus

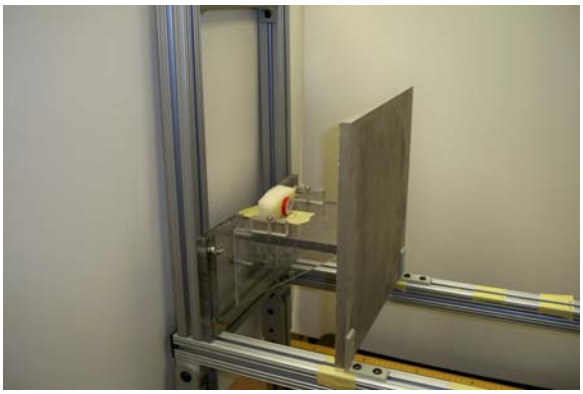

Figure 2: Source and Shielding

The aluminum frame measurement apparatus allowed consistent, reproducible and quick-set-up acquisitions at various distances from the source and with varying thickness and types of attenuation materials. Aluminum, iron and concentric hollow spheres made of tungsten powder (density of 11.0 g/cm) mixed with epoxy were used for the attenuating materials. A picture of the tungsten powder hemispheres and spheres are shown in Figure 3. The aluminum and iron attenuators were approximately 30 cm by 30 cm plates. The thicknesses of all attenuating materials ranged from 0.3 cm. to approximately 3 cm for each type of material.

All sources were type D capsules with a diameter of 25.4 mm and 6.35mm thick. Table 1 is a list of all sources used and their activities. The six sources that were used for energy calibration and detector characterization are indicated with an asterisk in the table. Background spectra were acquired when no apparent source was present and typically had total spectrum count rates of approximately 9,000 counts per minute. These are based on count rates observed in measured data

Figure 3: Tungsten Spheres

from the Identifinder. These rates include the ^{137}Cs calibration source inside the instrument detector.

Analysis

A sample set of measured gamma-ray spectra were analyzed using GADRAS. Each analysis required two spectra to be input, one for the spectrum acquired with a source present (foreground) and the other was its associated background spectrum (background). The first GADRAS analysis was performed with the automatic source identification function. The distance, foreground spectrum and

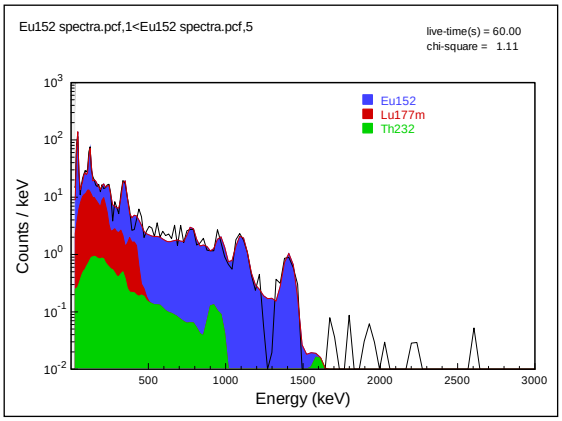

Figure 4a: Isotope I.D. Analysis Results

DateTime: 03-Mar-2010 13:03:51
TTF, TTB: 60, 60
Net Gamma: 160 cps
Net Neut.: 0 cps
SNM Prob.: 0 (Very Low)
Threat: 3 (Industrial)
ChiSquare: 1.1
Isotopes: Eu152(H,5uCi);Lu177m(F,1uCi)
Sigma Gam: 101
Sigma Neu: NA

Figure 4b: Isotope I.D. Analysis

the associated background spectrum are specified before performing the function. Figures 4a and 4b are screenshots of the automatic source identification results from this dataset. This function was run for each of the eleven sources with no shielding material between the source and detector, and with various amounts and types of shielding material. This function will list the isotopes identified in the order of certainty. In this case, ^{152}Eu was identified with high probability and ^{177m}Lu with a fair probability.

Table 2 is a compilation of results from data acquired for one minute live time. Column 2 shows the isotope that was used for the foreground gamma-ray spectrum and Column 3 shows the results from the identification function when no shielding material was placed between the source and detector. Columns 4, 5 and 6 are the results from shields with a half inch thickness of aluminum, iron and tungsten powder, respectively. Columns 7, 8 and 9 are the result with a one inch thickness of aluminum, iron and tungsten powder, respectively. The results in Table 2 show the isotopes identified with a letter in parenthesis that indicates a confidence level of high (H), fair (F) or low (L).

Table 2: GADRAS Source Identification Function Results

File Name	Isotope Present	No Shield Mtl.	Shield Mtl. 0.5 in. Al	Shield Mat. 1 in. Al	Shield Mtl. 0.5 in. Fe	Shield Mtl. 1 in. Fe	Shield Mtl. 0.5 in. W	Shield Mtl. 1 in. W	Comments
1	Am-241	Am-241(H)	Am-241(H)	Am-241(H)	None	None	None	None	W 1/4 and 3/8
2	Ba-133	Ba-133(H)	Ba-133(H); I-131(F)	Ba-133(H)	Ba-133(H)	Ba-133(H); Np-237(H)	Ba-133(H)	Ba-133(H)	W 1/4 and 1/2
3	Bi-207	Bi-207(H); U-238(F)	Bi-207(H); Cs-137(F)	Bi-207(H); Cs-137(H); U-238(F)	Bi-207(H); Cs-137(F)	Bi-207(H); Cs-137(F); U-238(F)	Bi-207(H)	Bi-207(H); Co-60(F)	W 3/8 and 7/8
4	Co-57	Co-57(H)	Co-57(H)	Co-57(H)	None	None	None	None	W 1/4 and 1/2
5	Co-60	Co-60(H); Se-75(F)	Co-60(H)	Co-60(H)	Co-60(H)	Co-60(H)	Co-60(H)	Co-60(H)	W 1/2 and 1
6	Cs-137	Cs-137(H)	Cs137(H); U235(H); Pu239(F)	Cs-137(H); Pu-239(F)	Cs-137(H)	Cs-137(H)	Cs-137(H)	Cs-137(H)	W 1/2 and 1
7	Eu-152	Eu-152(H)	Eu-152(H)	Eu-152(H); Am-241(F)	Eu-152(H); Am-241(F)	Eu-152(H); Th-232(F)	Eu-152(H)	Eu-152(H)	W 1/2 and 1
8	Mn-54	Mn-54(H)	Mn-54(H)	Mn-54(H)	Mn-54(H); Cs-137(F)	Mn-54(H); Ho-166m(F)	Mn-54(H)	Mn-54(H)	W 1/2 and 1
9	Na-22	Na-22(H)	Na-22(H); F-18(H)	Na-22(H)	Na-22(H)	Na-22(H)	Na-22(H)	Na-22(H)	W 1/2 and 1
10	Ra-226	Ra-226(H)	Ra-226(H); K-40(F)	Ra-226(H); I-131(F); Xe-133(F)	Ra-226(H); I-131(F)	Ra-226(H)	Ra-226(H)	Ra-226(H)	W 1/2 and 11/4
11	Th-228	Th-228(H); In-111(H); U-238(H); U-237(F)	U-232(H); In-111(H); Lu-177m(H); U-238(F)	U-232(H); Cs-137(H); In-111(H)	U-232(H); U-238(H); Lu-177m(F); U-235(L)	U-232(H); U-238(F)	None	Th232(H); K40(H); Cd109(H); U238(F)	W 1/2 and 11/4

The second analysis using GADRAS is a function to quantify the amount of radioactive material present. This function performs a single or multiple regression analysis after the appropriate elements are entered as shown in the screenshot in Figure 5a. Figures 5b and 5c show the results of the single regression analysis. A computed curve is overlaid on the measured spectrum (Figure 5b) and shows whether or not the curve fit is a good one. The source activity quantification results are shown in Figure 5c, which is 5.9 +/- 0.1 microcuries.

Figure 5a: Single Regression Analysis Setup

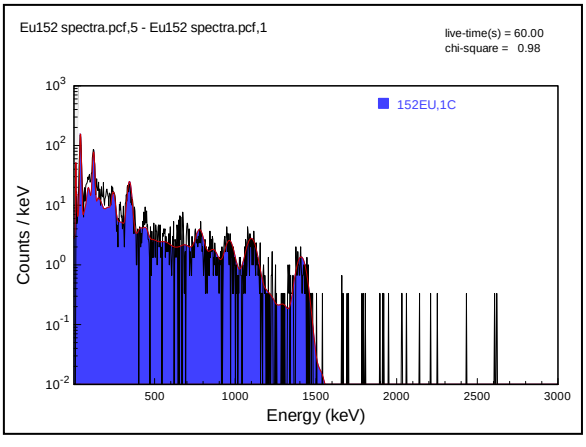

Figure 5b: Single Regression Analysis Curve Fit

```
********* SOURCE RANKING BY SINGLE REGRESSION ********

detector name      : SRNL Identifinder\Measured\Eu-152
distance (cm)      : 50
foreground spectrum: Eu152 spectra.pcf,5
background spectrum: Eu152 spectra.pcf,1
collect date/time  : 03-Mar-2010 13:22:45

Template        Chisqr      Amount      Units   AN    AD  Gain(%)

152EU            0.98     5.9 +/-  0.1   uCi  26.0   0.1    0.0
```

Figure 5c: Single Regression Quantification Results

The chi square value should be as low as possible and in this case is 0.98, indicating that the computed spectrum fits the actual spectrum very well. Also given in the results is a calculated atomic number (AN) and a calculated areal density (AD) for material such as shielding that might be present between the source and the detector. The source in this example was acquired with no shielding present, so AN is expected to be low and AD is near zero. The final value, the gain percent, shows how much the gain was shifted for this case.

GADRAS single regression analysis was performed for eight of the eleven isotopes and the results are listed in Table 3. These data consist of two groups of spectra. The larger group was acquired for 60 seconds live time. Each isotope was acquired unshielded and with three shielding materials, a half inch of aluminum, iron and a tungsten powder with a density similar to lead. The second group of data consisted of six isotopes that were acquired for long acquisition times. The results for each of these scenarios are given in Table 3.

Table 3: GADRAS Analysis of Single Isotope Spectra

Ground Truth			60 second Live Time Acquisitions												Long Count Data		
			No shielding			1/2" Al			1/2" Fe			1/2" W			No Shielding		
#	1st Isotope	uCi	Activity (uCi)	Unc.	% Diff.	Activity (uCi)	Unc.	% Diff.	Activity (uCi)	Unc.	% Diff.	Activity (uCi)	Unc.	% Diff.	Activity (uCi)	Unc.	% Diff.
1	Co-60	6.9	6.2	0.2	-10%	6.7	0.3	-3%	8	0.4	16%	7.8	0.5	13%	6.65	0.02	-3.5%
2	Co-57	3.9	2.8	0.1	-28%	2.94	0.06	-25%	2.5	0.2	-36%	--	--	--	4.47	0.05	14.6%
3	Ba-133	32.4	31.9	0.3	-2%	30.5	0.3	-6%	29.8	0.2	-8%	35.9	0.8	11%	30.7	0.1	-5.3%
4	Cs-137	46.2	41.5	0.3	-10%	45	1	-3%	36	1	-22%	36	4	-22%	46.5	0.2	0.7%
5	Am-241	50.2	43.1	0.9	-14%	53.7	1.1	7%	--	--	--	--	--	--	43.7	0.6	-12.9%
6	Eu-152	6.7	5.28	0.09	-21%	5.75	0.06	-14%	6.16	0.08	-8%	7.8	0.1	17%			
7	Bi-207	7.8	6.39	0.08	-18%	5.99	0.05	-23%	7.24	0.07	-7%	6.58	0.08	-15%			
8	Ra-226	10.7	13.9	0.1	30%	9.05	0.06	-16%	9.49	0.07	-12%	8.03	0.07	-25%			
Average percent deviation:					-9.1%			-10.1%			-10.8%			-3.6%			-1.3%

A final set of spectra that were acquired with two isotopes present were analyzed with the GADRAS multiple regression function and the results are shown in Table 4. These spectra were acquired for 60 seconds live time. The first section of the table gives the actual activity values of the two isotopes present. The second and third sections show the activity values calculated by GADRAS. For each measurement the activity, the uncertainty in the activity and the percent difference between the actual value and the calculated value is given.

Table 4: GADRAS Analysis of Spectra with Two Isotopes

Ground Truth					First Isotope			Second Isotope		
#	1st Isotope	uCi	2nd Isotope	uCi	Activity (uCi)	Uncert.	% diff.	Activity (uCi)	Uncert.	% diff.
1	Ba-133	32.2	Eu-152	6.7	29.8	0.5	-7.5	5.63	0.09	-15.7
2	Ba-133	32.2	Bi-207	7.8	31.8	0.5	-1.3	6.81	0.08	-12.1
3	Ba-133	32.2	Co-60	6.9	29.5	0.3	-8.5	5.6	0.05	-18.8
4	Ba-133	32.2	Ra-226	10.7	29.1	0.5	-9.7	8.5	0.07	-20.8
5	Ba-133	32.2	Co-57	3.9	34.7	0.3	7.7	2.72	0.1	-30.3
6	Eu-152	6.7	Bi-207	7.8	7.1	0.1	6.3	7.0	0.1	-9.7
7	Eu-152	6.7	Co-60	6.9	5.8	0.1	-13.2	5.8	0.1	-15.8
Average absolute percent deviation							-7.7			-17.6

RESULTS AND DISCUSSION

From Table 2 it can be seen that the GADRAS source identification function correctly identified the source with a high probability in 64 out of the 77 opportunities (83%). However, the thirteen isotopes incorrectly identified were either ^{241}Am, ^{57}Co or ^{228}Th. The first two had low energy gamma-rays and the third was a low activity source. The predominant gamma photons from ^{241}Am and ^{57}Co are approximately 60 and 122 keV, respectively, so they are expected to be attenuated with small amounts of shielding. The ^{228}Th source was relatively weak at 0.27 microcuries and its predominant gamma-ray energies are in the medium energy range at 238 and 583 kev. Also, these spectra were only acquired for 60 seconds to emulate real world situations so the total number of counts in the spectra is relatively small.

In many of the source identification results in Table 2 a second, third or fourth source is often listed as being present. GADRAS is able to determine isotopes that may be present in the spectrum that might be masked by other isotopes with stronger photopeaks as shown in the example in Figure 4a. The only isotope present in this example was ^{152}Eu, but ^{177m}Lu and ^{232}Th have photopeaks that could be located under the ^{152}Eu photopeaks. Notice in Figure 4b that the correct isotope, ^{152}Eu is identified with high confidence and ^{177m}Lu is given with only a fair confidence level. Further analysis with the multiple regression analysis can be done to investigate and rule out the presence of other isotopes. This feature of GADRAS offers an element of conservatism so the spectroscopist will consider more isotopes than those that are obvious at first glance.

Table 3 shows activity, uncertainty and percent differences for results of GADRAS single regression analysis using most of the isotopes listed in Table 1. Two columns represent calculated activities from unshielded sources for short and long acquisition times. The other columns show calculated activities from sources that are shielded with the three different material types and two different thicknesses. Comparing the two sets of data taken with no shielding, it can be seen that the results taken with long counting times are closer to the actual values and the uncertainties are smaller than the results from the 60 second

data. One should be careful when using isotopes with low radioactivity, resulting in poor counting statistics and larger deviations from the know values. Isotopes with similar radioactivities were compared in this study and the results were very favorable.

For the data in Table 3, the average absolute deviation was calculated for each category. As expected the best percent deviation was for the long count data (8.5%). The “no shielding” and aluminum shielding results were similar (32% and 29%) and the largest deviation from the known values was with iron (37%). The tungsten shield data was actually better than the data acquired for 60 seconds with no shielding, aluminum and iron. This can probably be explained because these shields, shown in Figure 3, are spheres that completely surround the source. This geometry would have the largest impact on the amount of backscatter photons that are detected. Reducing the backscatter has apparently increased the accuracy of the GADRAS calculation.

As shown in the Table 3 results for half-inch of iron shielding, there is a significant difference in the results for isotopes that are monoenergetic versus those that have several photon energies. For data acquired under similar conditions of source activity, count time, attenuating material and distance, GADRAS will calculate a better curve to fit the spectrum for an isotope with multiple energy photons than it will for a monoenergetic isotope. In Table 3 ^{133}Ba, ^{152}Eu and ^{207}Bi have percent differences of -8, -8 and -7, respectively. However, for the monoenergetic isotopes like ^{137}Cs, the percent difference is significantly larger (-22%). Generally, an isotope with several gamma-ray energies will result in a smaller chi square (better curve fit) than an isotope with only one photon energy because GADRAS is able to calculate the atomic number and areal density of the attenuation material more accurately. When multiple data points are used instead of just one, GADRAS is better able to determine the shielding characteristics and therefore the radioactivity of the source.

Variations in GADRAS results can also be attributed to the placement of shielding relative to the source and detector. The location of the shielding will affect backscatter differently and therefore the shape of the spectrum. Three configurations were used in this study: placing the shielding material next to the source, placing the shield next to the detector and using a spherical shield surrounding the source as was used with the tungsten powder spheres. GADRAS assumes the shielding around a source is in a four pi configuration. In this assumption, fewer counts are attributed to backscatter photons. In the aluminum and iron shielded cases, the shielding was a sheet of metal placed between the detector and the source. This non-spherical geometry caused some error in the GADRAS radioactivity estimate because backscatter photons are not accounted for accurately. The tungsten powder shield, however, was a hollow sphere and the source was placed inside the sphere to create a four pi

configuration. This is why the tungsten powder shielded cases have a lower average deviation (-3.6%) than the other shielding materials ~10%).

Table 4 shows results for spectra acquired for 60 seconds and containing two isotopes. The source-to-detector distance for the first isotope was 80-100 cm and the distance for the second isotope was 20-40 cm. These results show how distances between the source and the detector can significantly affect quantity calculations and the error in the measurement results. The percent difference results at short distances (isotope 2) are significantly greater than the results at longer distances (isotope 1). Some of the larger errors may be attributed to two isotopes being present but the distances probably play a larger role. At close distances there are greater variations in count rates that lead to greater uncertainty in the quantity calculation.

CONCLUSIONS

GADRAS is a great tool to efficiently identify isotopes and analyze gamma-ray spectra. An experienced gamma spectroscopist can quickly set up and analyze many gamma-ray spectra in minutes. The software performed well under challenging conditions of low count rates, varying detector-source distances and with different types and thicknesses of attenuating material. Hundreds of simulated gamma-ray spectra were created and many acquired spectra were analyzed using GADRAS as part of a recent NA-22 project. GADRAS results compare very favorably with other gamma-ray spectroscopy modeling and analysis tools[2]. This study shows the benefits of using GADRAS software and points out some caveats for its user to be aware of when using it.

ACKNOWLEDEMENTS

NA-22 Nonproliferation Detection Program
John Mattingly, Sandia National Laboratory
Dean Mitchell, Sandia National Laboratory
George Lasche, Sandia National Laboratory

REFERENCES

[1] Mitchell, D.J. and Waymire, D.R., *GADRAS User Manual*, Sandia National Laboratory, November 2009.

[2] Dewberry, R.A., Salaymeh, S.R., Brown, T.B., *Holdup Measurements on an SRNL Mossbauer Spectroscopy Instrument*, Submitted to J. Analytical and Nuclear Chemistry, 2010.

[3] Salaymeh, S.R., Jeffcoat, R.D., Clare, A., Owsley, L., Lorenz, C. and Alex Athey, A., Savannah River National Laboratory, University of Washington,

Johns Hopkins University and University of Texas, *Radioisotope Identification of Shielded and Masked SNM/RDD Materials*, 2010 INMM Annual Meeting.

[4] Owsley, L., Okopal, G., and Salaymeh, S.R., *New Directions in Radioisotope Spectrum Identification*, University of Washington and Savannah River National Laboratory, 2010 INMM Annual Meeting.

[5] Athey, A., and Salaymeh, S., *Spectral Relative Absorption Difference Method,* Applied Research Laboratories, The University of Texas at Austin, Savannah River National Laboratory, 2010 INMM Annual Meeting.

[6] Salaymeh, S. R.,.and Jeffcoat, R. D., *RadSonar Isotope Detection and Identification Algorithm Test and Evaluation Plan*, SRNL-L2200-2010-00036, Savannah River National Laboratory, March 8, 2010.